Case Studies in Construction Materials 7 (2017) 45–55

Contents lists available at ScienceDirect

Case Studies in Construction Materials

journal homepage: www.elsevier.com/locate/cscm

Case study

Awaso bauxite red mud-cement based composites: Characterisation for pavement applications

David Dodoo-Arhin[a,b,*], Rania A. Nuamah[a], Benjamin Agyei-Tuffour[a], David O. Obada[c], Abu Yaya[a]

[a] Department of Materials Science and Engineering, University of Ghana, Legon-Accra, Ghana
[b] Institute of Applied Science and Technology, University of Ghana, Legon-Accra, Ghana
[c] Department of Mechanical Engineering, Ahmadu Bello University, Zaria, Nigeria

ARTICLE INFO

Keywords:
Calcined red mud
Cement mortar
Bayer process
Portland cement
Compressive strength
Xrd

ABSTRACT

This paper presents the development of Bauxite residue (red mud) based cement composite mortar blocks for applications in pavement construction. The experimental techniques considered include the structural, thermal, morphological and microscopy analysis of the raw bauxite and red mud samples calcined at 800 °C. Composite mortar blocks of different batch formulations were produced and their physicochemical properties were investigated. The results show that the compressive strength of the as-prepared composite mortar blocks increased by ~40% compared to the type M mortar strength of ~2500 N/mm^2. The load bearing applications of the composites are discussed to influence the adoption of the calcined red mud as supplement in the production of low-cost Portland cement based composite mortar blocks for the construction industry.

1. Introduction

The search for recycling alternatives of several industrial wastes has become a very common practice aimed at reducing cost of industrial waste disposal and protection of the environment. One of such industrial waste is bauxite red mud; an alkaline leaching waste with typical pH of 10–13 [1–4], which is generated during the Bayer process or bauxite calcination method for alumina production [5–7].

Bauxite consists of ~75% of hydrated alumina ($Al_2O_3{\cdot}3H_2O$ and $Al_2O_3{\cdot}H_2O$) with the main impurities including iron oxide (goethite, $Fe_2O_3{\cdot}H_2O$), hematite (Fe_2O_3), anatase (TiO_2), rutile (TiO_2) and silicate impurities. The silicate impurities in bauxite are primarily quartz (SiO_2) and kaolinite. During the treatment of the bauxite ore by the Bayer process (Fig. 1), it is initially crushed and digested with a hot solution of sodium hydroxide (NaOH), and lime liquor at ≈175 °C and subjected to attack at high pressure and temperature. This condition makes it possible to convert the hydrated alumina into sodium aluminate solution (Eq. (1)), while the impurities remain in a solid state.

$$Al(OH)_{3(aq)} + NaOH_{(aq)} \xrightarrow[pressure]{Heat} AlO_2Na_{(aq)} + 2H_2O \quad (1)$$

The impurities are separated from the aluminate solution by decantation and filtration, followed by washing. The solid residues thus obtained are called red mud and are mainly made up of oxides of iron, aluminium, silicon and titanium. However, despite being

* Corresponding author at: Department of Materials Science and Engineering, University of Ghana, Legon-Accra, Ghana.
E-mail addresses: ddarhin@yahoo.com, ddodoo-arhin@ug.edu.gh (D. Dodoo-Arhin).

http://dx.doi.org/10.1016/j.cscm.2017.05.003
Received 28 December 2016; Received in revised form 22 March 2017; Accepted 17 May 2017
Available online 15 June 2017

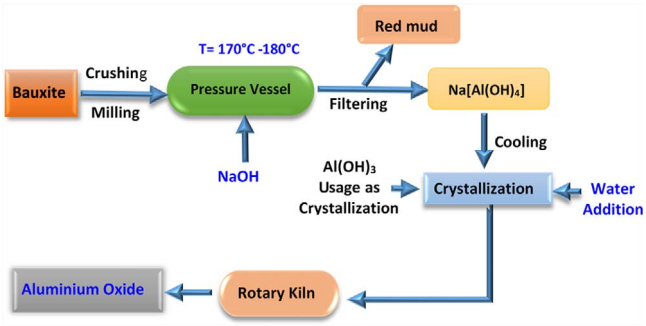

Fig. 1. The Bayer process of red mud and alumina production.

washed and considered as an inert solid waste, red mud remains strongly alkaline and highly corrosive. It is usually discharged as highly alkaline slurry (pH 10–13.5) with 15–40% solids, which is pumped away for appropriate disposal. This strong alkaline character (Na_2O + NaOH = 2.0–20.0 wt.%), restricts the disposal conditions of red mud in order to minimize environmental problems such as soil contamination and ground water pollution. Its chemical and mineralogical composition may however slightly vary, depending on the source of bauxite, the technological processing conditions (Bayer process or bauxite-calcination method) and storing ages. It is composed of six major oxides (Al_2O_3, Fe_2O_3, Na_2O, SiO_2, CaO, and TiO_2), and a large variety of other minor elements.

It has been estimated that 66 million tons of red mud [8] is produced annually across the world and it is considered to be "hazardous" according to the Brazilian NBR 10004 standard [9]. Over the years, the disposal of red mud by methods such as sea water discharge, lagooning and dry- stacking has been a major challenge to alumina companies and environmentalist. It is expensive, requires lot of land and poses numerous environmental and health hazards. As a result of these challenges, lots of research has been carried out to device means of economically utilizing this highly alkaline waste as a raw meal for the production of Portland cement clinker, as a partial substitute for clay in the production of bricks [10], in the preparation of special cements [11] and pozzolanic pigment.

Portland cement happens to be one of the most popular and widely used building materials across the world due to the availability of raw materials over the world, easy processing and its amenability to conceivable shapes [12]. However, there are two major drawbacks with respect to sustainability in the use of Portland cement which are: (1) about 1.5 tons of raw materials is needed in the production of every ton of Portland (PC), at the same time also about one ton of carbon dioxide (CO_2) is released into the environment which means that the production of Portland cement is a resource and energy intensive process. (2) Concretes made of Portland cement deteriorate when exposed to severe environments and this affects the service behaviour, design life and safety of structural constructions [13]. Studies have shown that utilization of red mud in the production of construction and building materials has the potential of consuming the red mud waste in higher quantities. For instance, it was reported that 2.5 million tons of red mud was consumed by the cement industry during 1998–1999 in India and researchers found that the hydration reaction of Portland cement is favoured by a highly alkaline environment which red mud is noted for [14]. The high alkalinity of red mud which is of environmental concern serves as a major asset in the attempt of inhibiting corrosion in reinforced concrete rebar and reducing sulphur build-up in the kiln system of cement plants. Tsakiridis et al., [11] in Greece studied the addition of red mud residue by 1% in the raw mix for the production of Portland cement and found that the red mud can be utilized as a raw material in cement production, at no cost to the producer thus, contributing in the reduction of the process cost. It has also been found out that the maximum potential strength developed by cement is never fully utilized as about half of the amount of Portland cement consumed in building construction is used in masonry and plastering whose strength requirement is about 4.0 MPa while Portland cement is suited for applications with strength requirements exceeding 15.0 MPa [15]. Materials with pozzolanic characteristics may thus be used to partially replace the cement in those applications and red mud is tested here for this purpose.

This study investigates the physico-mechanical and economic influence of calcined Bayer red mud addition in Portland cement based pavement blocks.

2. Experiment

2.1. Materials and methods

2.1.1. Bayer red mud sample preparation and characterisation

The bauxite for the red mud preparation was obtained from Awaso in the western region of Ghana (Fig. 2) which is the main bauxite occurrence in Ghana. The bauxite rests on a layer of kaolin or lithomarge, which separates it from the underlying slates and the lower Birimian phyllites which strikes at N40E to N80E with steep dips to the NW. Hence, this bauxite can be classified as lateritic silicate bauxite because they have been formed as a result of indirect bauxitization processes under tropical weathering conditions. The built up sections range from the top soil, Bauxite and to Lithomargic clay (rock like) occurrences.

In a typical red mud production via the Bayer process, ball milled bauxite with particle sizes < 355 μm were slurred with hot (135 °C–140 °C) 2 M concentration of NaOH and digested in a 1L pyrex beaker at atmospheric pressure under constant stirring for

Fig. 2. Geological map of Ghana showing the Awaso bauxite deposits site.

~30 min to enable dispersion of particles. After digestion, the homogenous mixture was allowed to cool to room temperature for 24 h and the liquid aluminous is filtered off leaving the residue on a filter paper (Fig. 3).

The chemical and mineralogical composition of the samples was determined using a Thermo Fisher ARL9400 XP+ Sequential XRF equipped with WinXRF software for analyses. The samples were milled in a tungsten-carbide milling pot to achieve particle sizes < 75 μm and dried at 100 °C. After drying, the samples were roasted at 1000 °C to determine loss on ignition (LOI) values. 1 g of the sample was mixed with 6 g lithium tetraborate flux ($Li_2B_4O_7$) and fused at 1050 °C to make a stable fused glass bead. For trace element analyses, the sample was mixed with a PVA binder and pressed into a pellet using a 10-ton press.

X-ray powder diffraction (XRD) patterns were collected on an XPERT-PRO diffractometer (PANalytical BV, Netherlands) with theta/theta geometry, operating a cobalt tube at 35 kV and 50 mA. The goniometer is equipped with automatic divergence slit and a PW3064 spinner stage. The X-ray diffraction patterns of all specimens were recorded in the 10°–70° 2θ range with a step size of 0.017° and a counting time of 14 s per step. Qualitative phase analysis was conducted using the X'Pert Highscore plus search match software.

The morphology of the samples was studied on a FEI XL 30 Environmental Scanning Electron Microscope equipped with an Energy Dispersive X-ray Spectroscopy system based on a nitrogen cooled Si-Li detector. The samples were metalized and analyzed at 30 kV and 93 μA.

The thermal stability of the various phases in the samples was studied on a standard SDT Q600 (V20.9 Build 20) TG/DTA instrument under air flow of 50 mL/min. Prior to analysis A sapphire standard was used to calibrate the thermal response due to heat flow as well as the temperature. 25 mg of the specimens were placed in an alumina (Al_2O_3) crucible (100 mg capacity), subjected to a linear heating ramp between 15 °C and 1200 °C at a rate of 10 °C/min and a cooling rate of 50 °C/min. The test measurements were

Fig. 3. Materials used; (a) river sand as fine aggregates; (b) ordinary Portland cement (Diamond, class 42.5N); (c) Bauxite red mud and (d) red mud cement composite.

made for the mass change (loss) of the sample as a function of the temperature and the phase changes by the adsorption or the emission of energy.

2.2. Bauxite red mud- cement composite mortar pavement blocks fabrication

The mortar was prepared using a Ghanaian limestone Portland cement (Diamond class 42.5N), calcined red mud, fine aggregates (river sand) and laboratory tap water. The red mud from the Bayer process was calcined for 2 h at 800 °C in a gas test kiln in order for the aluminium hydroxides (boehmite and gibbsite) to develop some pozzolanic behaviour [16,17]. The control mix proportion for the mortar preparation was Portland cement, sand and 0.5 water/cement ratio according to the BS EN196-1: 1995 standard. The materials were weighed into the mixer bowl which mixes the materials into a homogenous mixture whiles a measured amount of water is poured into the mix simultaneously to form the paste.

The stirrer of the mixer was set to rotate at a speed of 4 rpm and the total time used for mixing each batch was 120 s. The quantity of the sand and water were kept constant while that of the cement was varied with red mud in the percentages of 5, 10, 15, 20 and 25. Table 1 gives an illustration of the design mix proportion and the batch formulation respectively.

Four 7.5 cm × 7.5 cm cubes, 6 cm × 3 cm × 2 cm briquettes and 20 cm × 1 cm × 1 cm bar samples were made from each mix batch as shown in Fig. 4.

Table 1
Batch formulation.

Sample	Red Mud replacement (%)	Fine Aggregate (sand) (Kg)	Cementitious materials (Kg)		Remarks
			Portland cement	Red mud	
BRC-0	0	2.000	1.000	0.000	Reference
BRC-1	5	2.000	0.950	0.050	5%RM
BRC-2	10	2.000	0.900	0.100	10%RM
BRC-3	15	2.000	0.850	0.150	15%RM
BRC-4	20	2.000	0.800	0.200	20%RM
BRC-5	25	2.000	0.750	0.250	25%RM

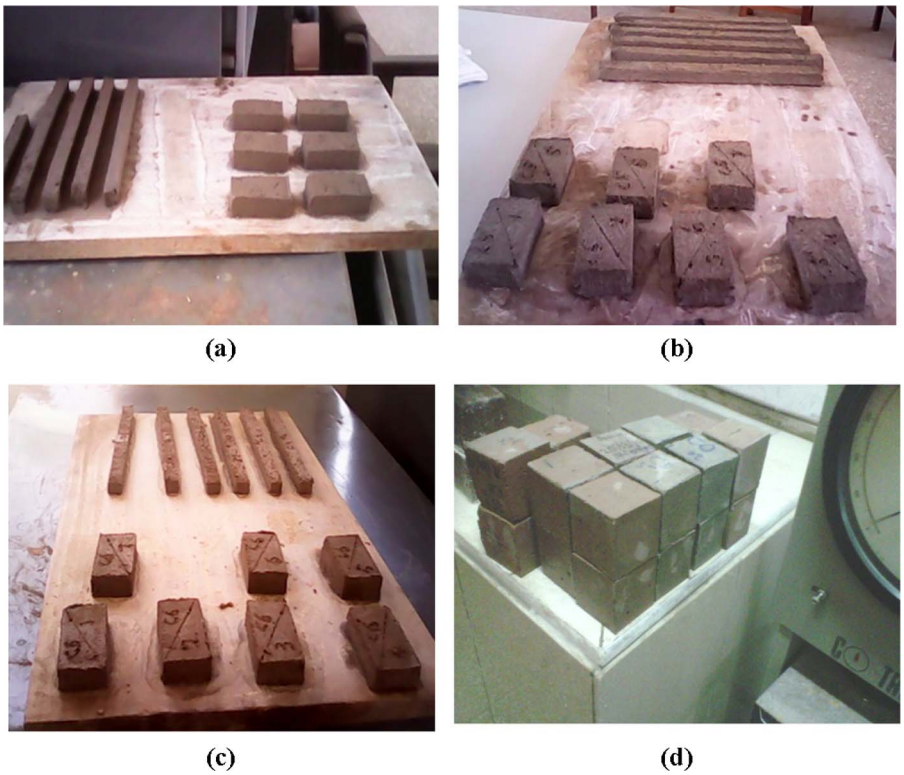

Fig. 4. Bauxite Red Mud-Cement batch samples; (a) OPC bars and brickettes, (b) 5% Red mud, (c) 20% Red mud and (d) RMC Mortar cubes.

2.3. Physical property characterization

The standard consistency, the initial and final setting times of the fresh red mud – Cement based mortar of the various batches were determined using the Vicat needle apparatus (Controls, L28) according to the British and European Standards BS EN 196-3:1995

The water of absorption characterisation was conducted to estimate the final products' (blocks) susceptibility to seepage of water through its pores when immersed in water. The average weight of a fired briquette was measured in air and then re-weighted after being soaked in water for about one hour. The water of absorption (WA) values were obtained in relation to the apparent porosity (AP) and bulk density (BD) as given in Eqs. (2)–(4), respectively.

$$WA(\%)=\frac{S_w\text{-}F_w}{F_w}x100 \tag{2}$$

$$AP(\%)=\frac{W_c\text{-}W_a}{W_c\text{-}W_b}x100 \tag{3}$$

$$BD = \frac{W_a}{W_c - W_b} \tag{4}$$

S_w is the soaked weight, F_w is the fired weight, W_a is the sample dry weight in air, W_b is the weight of soaked sample in water, and W_c is the weight of soaked sample measured in air.

ASTM C830-09 and ASTM D6111-09 standard tests were followed in the determination of the porosity and bulk density respectively. The apparent and bulk density tests were carried out by making briquettes of 6 cm × 3 cm × 2 cm samples. After demoulding, their wet weights (W_w) were taken and subsequently conditioned in the laboratory for 24 h. After conditioning, the dry weight (W_d) of the samples were taken after which the samples were totally immersed in water for 28 days to ensure that the pores of the samples were completely filled with water. After the 28 days the samples were taken out and weighed in order to determine the weight soaked in air (W_s) after which the soaked samples were suspended in water and the weights taken (W_{ss}). The apparent porosity and bulk density was determined using the Archimedes principle.

Water absorption data and apparent porosity variation as the content of red mud increases are presented and discussed.

2.4. Flexural strength (modulus of rapture-MOR)

Using three-point bending testing (ASTM C99/C99M-09 standard protocols), the flexural strength of the test bars was determined. Fig. 5 represents the test configuration for specimen dimension of 20 × 1 × 1 cm^3 and distance 7.6 cm (between supports).

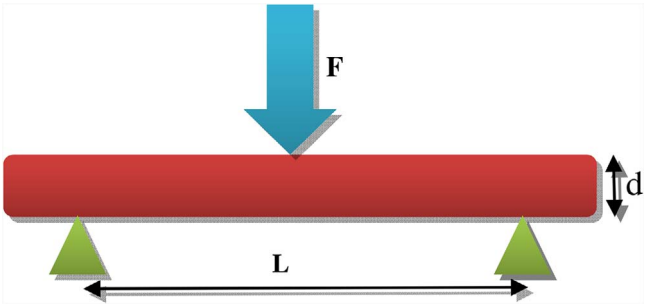

Fig. 5. Schematic Three-Point Bending Method.

Table 2
Chemical composition of bauxite and red mud estimated by XRF.

Major oxides	Awaso Bauxite (%)	Awaso red mud (%)
Al_2O_3	65.15	51.07
SiO_2	2.75	2.15
Fe_2O_3	6.99	7.15
Na_2O	1.05	2.84
TiO_2	1.93	1.77
CaO	0.06	1.07
MgO	0.08	0.22
P_2O_5	0.15	0.15
SO_3	0.13	0.10
K_2O	0.04	0.04
MnO	0.01	0.01
L.O.I	23.08	33.9

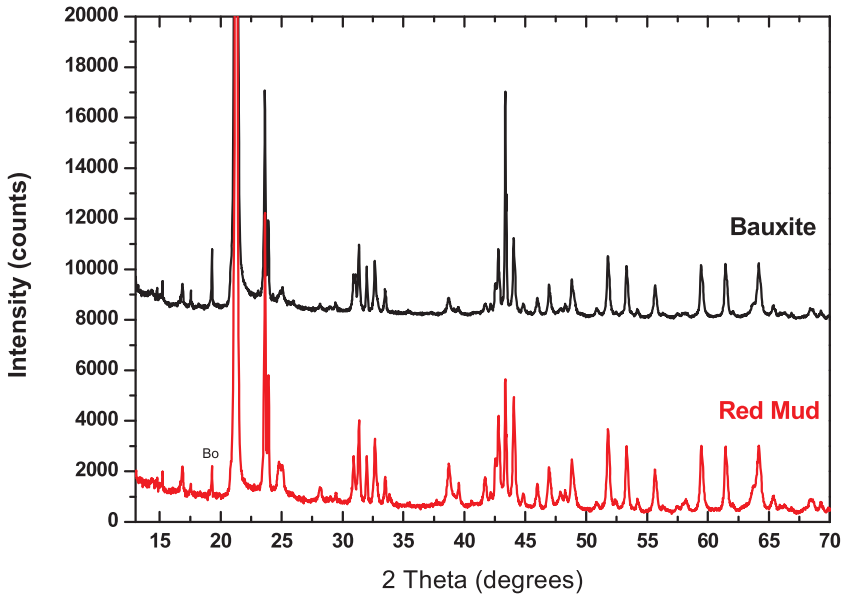

Fig. 6. XRD pattern of Awaso bauxite and red mud.

Monotonic loading was done at 1.85 kg/min till point of fracture. Eq. (5) was used in computing flexural strengths and the average values were recorded from two tests. The effect of the percentage red mud content on the flexural strength values was investigated.

$$\sigma = \frac{3FL}{2dh^2} \tag{5}$$

Where F is load, b is breadth, h is depth, L is distance between supports used.

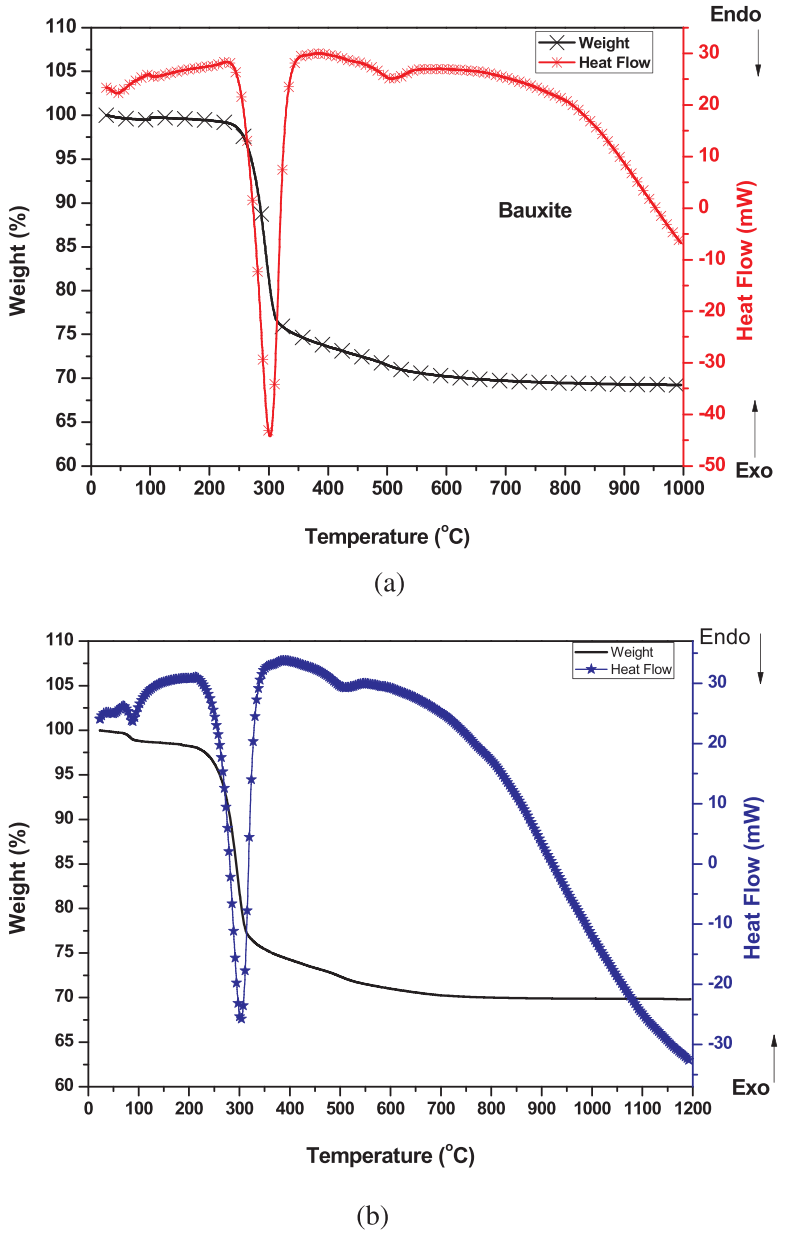

Fig. 7. Tg (Wt%)-DTA (Heat flow) thermographs of (a) Awaso Bauxite, and (b) Awaso Red mud.

3. Results and discussion

3.1. XRF and XRD analysis

The mineralogical composition as well as physical and chemical properties has a critical influence on the industrial applications of ceramic materials. From Table 2, it can be seen that the dominant oxide in the Awaso red mud is Al_2O_3. It is also worth stating that the dominant red colour of both the red mud and bauxite is attributed to the well dispersed particles of iron oxide (Fe_2O_3) in both samples.

From the XRD data (Fig. 6), the main mineral phases identified in the Awaso red mud sample using the X'Pert Highscore plus software are hematite (Fe_2O_3, card no.33-0664), rutile (TiO_2, card no. 21-1276), perovskite ($CaTiO_3$, card no. 22-1053), quartz (SiO_2, card no. 18-1166), sodalite ($Na_2O{\cdot}Al_2O_3{\cdot}SiO_2$, card no. 16-0612), boehmite {AlO(OH), card no. 21-1307}, goethite {FeO (OH), card no. 26-0792}, gibbsite {$Al(OH)_3$, card no. 33-180}, calcium alumina silicate {$Ca_2Al_2(SiO_4)(OH)_8$, card no. 03-0798}.

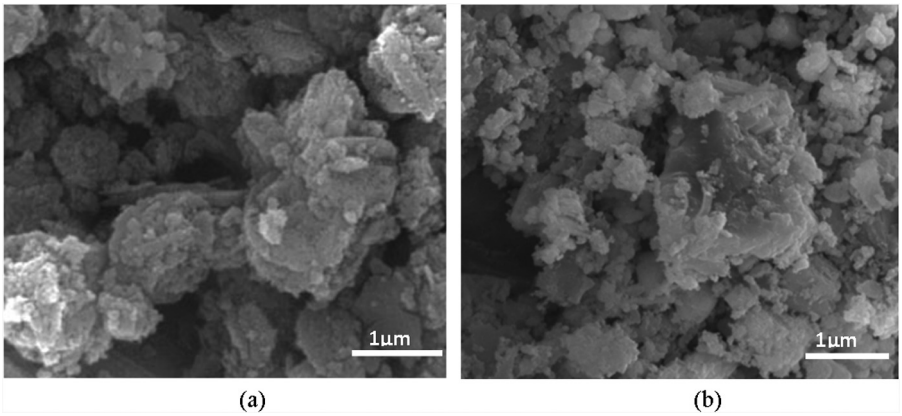

Fig. 8. SEM images of (a) Calcined Red Mud and (b) Red Mud-Cement composite.

Table 3
Physical and Mechanical Properties of RMC blocks.

Sample	Standard consistency	Initial setting time (mins)	Final setting time (mins)	Flexural strength (Kg/cm^2)	Compressive strength (N/mm^2)	Bulk density (g/cm^3)	Apparent Porosity (%)	Water absorption (%)
BRC-0	24.00	176	379	55.84	43.20	2.18	2.65	0.96
BRC-1	25.00	134	364	57.85	43.00	2.22	0.45	1.11
BRC-2	27.00	132	335	43.48	35.98	2.22	1.13	2.20
BRC-3	30.00	126	201	43.66	32.65	2.19	1.36	2.60
BRC-4	32.00	100	172	39.17	31.88	2.15	2.74	3.57
BRC-5	36.00	95	212	34.87	27.90	2.15	4.04	7.70

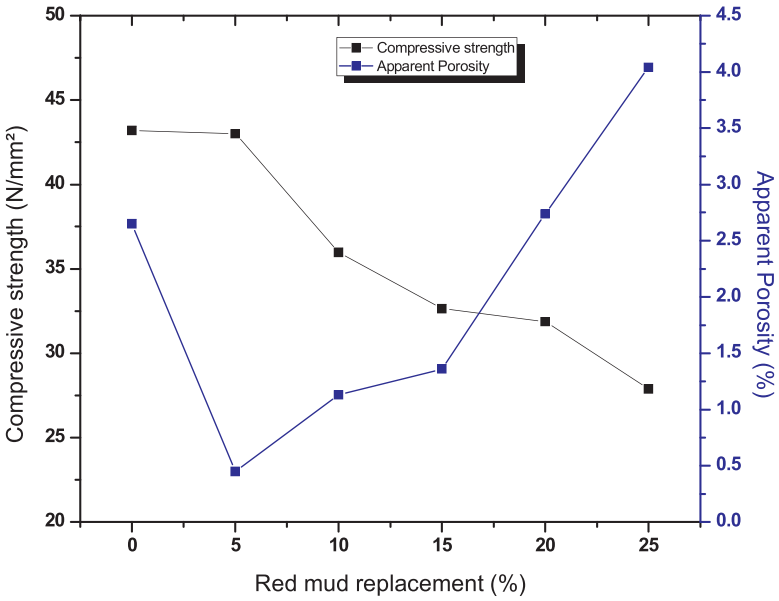

Fig. 9. Relationship between apparent porosity and compressive strength with red mud replacement.

3.2. Thermal analysis (TG-DTA)

The main mineral phases of dried red mud at room temperature are calcite ($CaCO_3$), dicalcium Silicate (Ca_2SiO_4), hematite (Fe_2O_3), perovskite ($CaTiO_3$), gibbsite ($Al(OH)_3$), and CaO. The TG-DTA thermograms (Fig. 7) show a continuous weight loss distributed in the range of 25–1200 °C. The figure shows two main portions of mass loss as the rise of temperature. The first one is during the heating temperature interval of 50–550 °C when the physically absorbed water and chemically bound water is off. Before the temperature gets up to 500 °C, the sample loses ≈27.62% of its total weight. The proportion of physically absorbed water is small.

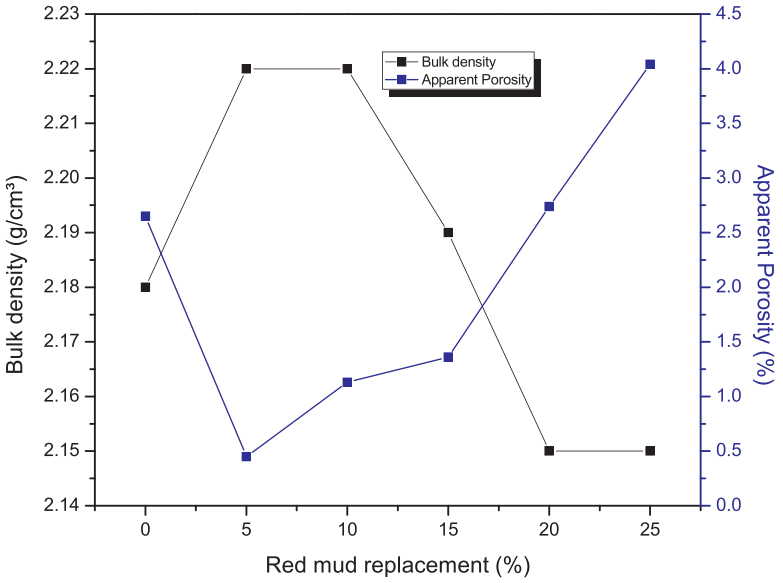

Fig. 10. Relationship between bulk density and apparent porosity with red mud replacement.

Comparing this result with the results of the XRD analysis, the lost chemically bound water could be mainly attributed to the decomposition of gibbsite ($Al(OH)_3$) to alumina (Al_2O_3) and H_2O which can combine with the CaO to form tricalcium aluminate or Gehlenite.

The more rapid decline in the range of 550–900 °C with a mass change of ≈1.81% could be attributed to the release of CO_2 [18]. The release of CO_2 is due to the decomposition of Calcite ($CaCO_3$) into CaO. The chemical equations during this phase transformation are as follows:

$$CaCO_3 \rightarrow CaO + CO_2,\ 3CaO + Al_2O_3 \rightarrow Ca_3Al_2O_6, \quad (6)$$

$$2CaO + 2Al_2O_3 + SiO_2 \rightarrow 2Ca_2Al_2SiO_7. \quad (7)$$

The phases of tricalcium aluminate ($Ca_3Al_2O_6$) and gehlenite ($Ca_2Al_2SiO_7$) start to develop in the 800–900 °C range. There is no obvious mass change or phase change above 900 °C.

The SEM micrographs (Fig. 8) of the red mud and red mud-cement composites show particles with plate-like shapes and agglomerates on the microstructure scale which could be attributed to the processing of the powders via ball milling. Homogeneous blend of the red mud and cement for the various batches were physically observed.

3.3. Physical and mechanical properties of red mud cement mortar blocks

From Table 3, it is observed that both the initial and final setting times of the Portland cement mortar decreases with increase in red mud additions thus, the addition of red mud tends to accelerate the setting process. This result can be attributed to the high alkalinity of the red mud and the presence of aluminium and sodium hydroxides (known as curing accelerators).

The standard consistency of the mortar samples increases as the amount of calcined red mud increases as shown in Table 3. This observation can be attributed to the fact that the red mud particles are lighter, finer and occupy large volume hence the amount of water needed to obtain the same standard paste as compared to the reference mortar increases. Also, as the red mud content increases, the workability of the paste decreases and more water is needed for the wetting and kneading of the paste.

It can be seen from Table 3 that the flexural strength value decreases for mortars with red mud percentages of 10, 15, 20 and 25 and value increases for 5% red mud replacement in cement with respect to the reference mortar. This decrease in strength could be attributed to the fact that as the red mud content increases, the workability decreases and the packing effect reduces thereby causing the material to be porous and having reduced strength. However, for 5% red mud replacement it could be seen from the table that the flexural strength was higher than that of the reference mortar block and this could be attributed to the fact that the bonding between the particles was very strong due to better packing hence the increase in strength.

It can be observed from Fig. 9 that as the red mud content increases the compressive strength decreases. The strength of the mortar block is affected by the workability and the porosity and as deduced earlier, the increase in red mud content tends to decrease workability and increase porosity. From these inference it can be said that the more the red mud content the less the strength.

It can be seen from Fig. 10 that for 5%, 10% and 15% red mud replacement, the bulk density increases as compared to the reference mortar block. This is due to the fact that with these replacements, the fine nature of red mud increased mortar compactness thus producing high density (filler effect). However, for subsequent increase in red mud, because of the decrease in workability, the

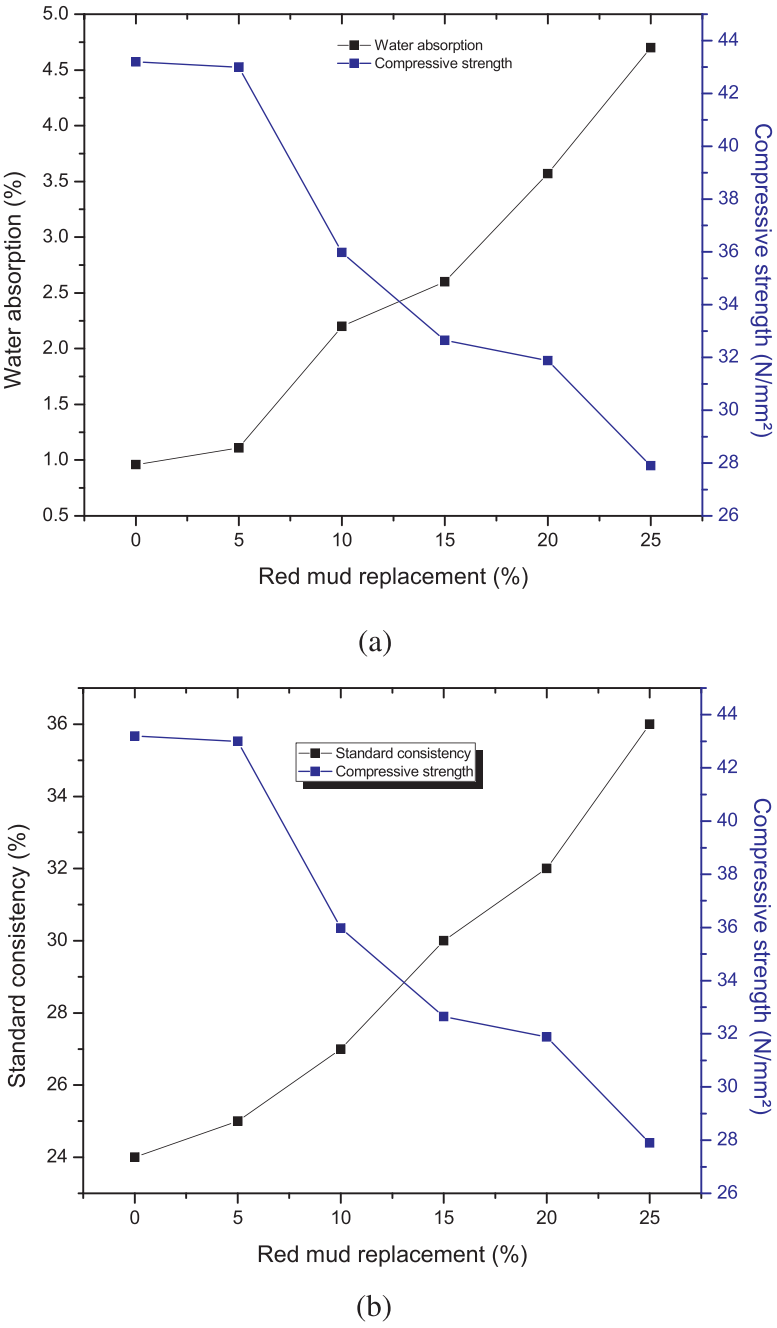

Fig. 11. Effect of red mud replacement on the (a) water absorption-compressive strength (b) Standard consistency – Compressive strength relationships.

mortar compactness is less hence decreases density. It can also be seen that as the density increases, porosity decreases and as porosity increases density decreases.

It can be seen from Fig. 10 that as the red mud content increases in the mortar, the water absorption also increases. This observation can be attributed to the fact that as the Red mud (RM) content increases the workability decreases and as the workability decreases the porosity increases, hence the amount of water that is able to seep through the pores increases.

For water of absorption to increase, it means a material is porous and from Fig. 11a, increasing red mud addition to cement mortar increases the porosity due to reduced workability and increase porosity and water absorption degrades the strength of the mortar. This also increases the standard consistencies (Fig. 11b) of the mortars.

Mortar blocks for paving applications are more likely to be in a saturated condition than those for walls. In view of this, the mortar typically must be more durable to resist the harsher exposure. Type M mortar is recommended with Type S as the alternate. In general, comparing the compressive strengths of the various compositions of red mud based mortars with ASTM C 270 classification

of mortar, the red mud based mortars can be classified as a type M (high strength and for load bearing applications) composite mortar blocks [19,20].

4. Conclusions

Generally, increase in calcined red mud content decreases the compressive as well as flexural strength. However, 5% red mud additions tend to have superior or equal qualities to the reference mortar. Workability of mortar generally is decreased with the increase in red mud content and both the initial and final setting times are accelerated mostly due to the presence of aluminium and sodium hydroxides (curing accelerators). The addition of calcined red mud at 800 °C tend to increase the bulk density and decrease porosity for red mud percentages of 5, 10 and 15. The rate at which water seep through the pores (water of absorption) of the mortar blocks also tends to increase with the increase in red mud addition and this has a negative influence on the strength of the mortar block. The replacement of Portland cement with RM up to 25% in mortar preparation for pavement blocks application as achieved in this study would help reduce cost, reduce the impact of the Bayer red mud waste on the environment and also reduce the depletion of the raw materials needed to produce cement which will in turn reduce the amount of CO_2 released into the environment. To improve the workability of the red mud based mortars, super plasticizers such as polycarboxylate ether and melamine sulfonate may be added.

Acknowledgement

Authors acknowledge the University of Ghana, University of Pretoria and the Ghana Standards Authority for support.

References

[1] S.S. Amritphale, M. Patel, Utilisation of red mud, fly ash for manufacturing bricks with pyrophyllite, Silic. Ind. 2 (1987) 31–35.
[2] Building Code Requirements for Masonry Structures (ACI 530/ASCE 5/TMS 402) and Specification for Masonry Structures (ACI 530.1/ASCE 6/TMS 602), The Masonry Society, Boulder, CO, 2005.
[3] F. Habashi, Bayer's process for alumina production: a historical perspective, Bull. Hist. Chem. 17 (1995) 18.
[4] A.R. Hind, S.K. Bhargava, S.C. Grocott, The surface chemistry of Bayer process solids: a review, Colloids Surf. A.: Physicohem. Eng. Aspects 146 (1–3) (1999) 347–359.
[5] C. Lin, G. Maddocks, J. Lin, G. Lancaster, C. Chu, Acid neutralizing capacity of two bauxite residues and their potential applications for treating acid sulphate soil and water, Aust. J. Soil Res. 42 (5–6) (2004) 649–657.
[6] D.Y. Liu, C.S. Wu, Stockpiling and comprehensive utilization of Red Mud, Materials 5 (2012) 1232–1246.
[7] Z. Li, Z. Ding, Y. Zhang, Development of sustainable cementitious materials, Proceedings of the International Workshop on Sustainable Development and Concrete Technology, Beijing, China, 2004, pp. 55–76.
[8] H. Mahadevan, H.K. Chandwani, P.M. Prasad, An Appraisal of the Methods for Red Mud Disposal Under Indian Conditions, Allied Publishers, New Delhi, 1996, pp. 337–347.
[9] P.K. Mehta, Advancements in concrete technology, Conc. Int. 21 (6) (1999) 69–76.
[10] P.K. Mehta, P.C. Aïtcin, Principles underlying the production of high-performance concrete, Cem. Concr. Aggreg. ASTM 12 (2) (1990) 70–78.
[11] N.W. Menzies, I.M. Fulton, W.J. Morell, Seawater neutralizing of alkaline bauxite residue and implications for revegetation, J. Environ. Qual. 33 (2004) 1877–1884.
[12] V. Pascale, D.T. Rajeshwar, C.A. Jean, J.W. Kevin, Chemical and biological leaching of aluminum from red mud, Environ. Sci. Technol. 28 (1) (1994) 26–30.
[13] J. Pera, A. Motazi, Pozzolanic activity of calcined red mud. Proceedings of the 4th CANMET/ACI International Conference on Fly Ash. Silica fume, Slag and Natural Pozzolans in Concrete. Istanbul, Turkey, V.M Malhotra, (ed.) SP 1992; 132[749]:132.
[14] J. Pera, R. Brumaza, J. Ambroise, Development of a pozzolanic pigment from red mud, Cem. Conc. Res. 27 (10) (1997) 1513–1522.
[15] R.N. Summers, J.D. Pech, Nutrient and metal content of water, sediment and soils amended with bauxite residue in the catchment of the Peel Inlet and Harvey Estuary, Western Australia, Agr. Ecosyst. Environ. 64 (1997) 219–232.
[16] P.E. Tsakiridis, S. Agatzini-Leonardou, P. Oustadakis, Red mud addition in the raw meal for the production of Portland cement clinker, J. Hazard. Mater. B116 (2004) 103–110.
[17] Technical Notes on Brick Construction-8B: Mortars for Brickwork – Selection and Quality Assurance, Brick Industry Association, Centennial Park Drive, Reston, Virginia, 2006, pp. 1–6.
[18] M.S. Vincenzo, C. Renz, M. Stefano, C. Giovanni, Bauxite red mud in the ceramic industry, part 2: production of clay based ceramics, J. Eur. Ceram. Soc. 20 (2000) 245–252.
[19] M.R. Yogananda, K.S. Jagadish, Pozzolanic properties of rice husk, burnt clay and red mud, Build. Environ. 23 (4) (1998) 303–308.